

# Organic & Biomolecular Chemistry

Accepted Manuscript



This is an *Accepted Manuscript*, which has been through the Royal Society of Chemistry peer review process and has been accepted for publication.

*Accepted Manuscripts* are published online shortly after acceptance, before technical editing, formatting and proof reading. Using this free service, authors can make their results available to the community, in citable form, before we publish the edited article. We will replace this *Accepted Manuscript* with the edited and formatted *Advance Article* as soon as it is available.

You can find more information about *Accepted Manuscripts* in the [Information for Authors](#).

Please note that technical editing may introduce minor changes to the text and/or graphics, which may alter content. The journal's standard [Terms & Conditions](#) and the [Ethical guidelines](#) still apply. In no event shall the Royal Society of Chemistry be held responsible for any errors or omissions in this *Accepted Manuscript* or any consequences arising from the use of any information it contains.

Cite this: DOI: 10.1039/c0xx00000x

www.rsc.org/xxxxxx

ARTICLE TYPE

# DFT Studies on the Directing Group Dependent Arene-Alkene Cross-Couplings: Arene Activation vs. Alkene Activation

Lei Zhang,<sup>a</sup> and De-Cai Fang<sup>\*a</sup>

Received (in XXX, XXX) Xth XXXXXXXXXX 20XX, Accepted Xth XXXXXXXXXX 20XX

DOI: 10.1039/b000000x

Abstract: As its green-chemistry advantages, the dehydrogenative Heck reaction (DHR) has experienced enormous growth over the past decades. In this work, two competing reaction channels were comparatively studied for the Pd(OAc)<sub>2</sub>-catalyzed DHRs of arenes with alkenes, referred to herein as arene activation mechanism and alkene activation mechanism, respectively, which mainly differ in the involvement of the reactants in the C-H activation step. Our calculations reveal that the commonly accepted arene activation mechanism is plausible for the desired arene-alkene cross-coupling; in contrast, the alternative alkene activation mechanism is kinetically inaccessible for the desired cross-coupling, but it is feasible for the homo-coupling of alkenes. The nature of directing groups on reactants could mainly determine the dominance of the two competing reaction routes, and therefore, influence the experimental yields. A wide range of directing groups experimentally used are examined by the density functional theory (DFT) method in this work, providing a theoretical guidance for screening compatible reactants.

## Introduction

The Pd-catalyzed Heck reaction<sup>[1]</sup> has been widely used as a reliable and versatile C-C cross-coupling methodology, especially for the syntheses of arylalkenes from aryl halides and alkenes. In contrast to the classical Heck reaction using organic halides as substrates, the dehydrogenative Heck reaction<sup>[2]</sup> (DHR) is more atom-economy, since the result of DHR is direct formation of a C-C bond from an arene and an alkene. It has been therefore a research focus of organic synthesis since 2000<sup>[3]</sup>, with particular attention to expansion of substrate scope, improvement of reaction efficiency and reduction of catalyst loadings, etc.

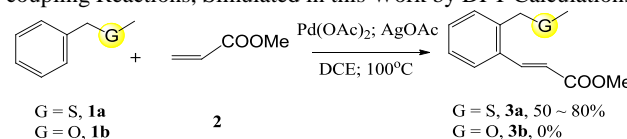
The determinants of experimental yields might be complicated and manifold, which sometimes include modulations of catalytic species<sup>[4]</sup>, reaction solvents<sup>[5]</sup>, additives<sup>[6]</sup> and reoxidants<sup>[7]</sup>. Extensive investigations revealed the key role played by oxidative systems; for example, Yu and co-workers<sup>[8]</sup> disclosed the *mono*-alkenylation of phenylacetic acids was efficient when using a catalytic amount of benzoquinone associated with O<sub>2</sub>. Subsequently, the same research team isolated the dialkenylated phenylacetic acids merely by replacement of benzoquinone with AgOAc<sup>[9]</sup>.

DHRs might proceed through multiple reaction mechanisms proposed previously depending on the catalytic conditions, in which the involvement of a discernible  $\sigma$ -arylpalladium(II) intermediate, formed from the C-H activation of aromatic substrates with Pd<sup>II</sup>-catalysts, was generally accepted<sup>[2,10]</sup>. For regioselective purpose, arenes functionalized with appropriate directing groups were the main materials used to achieve *ortho* palladation<sup>[11]</sup>. A series of O-containing groups<sup>[12]</sup> are the most prevalent in the directed C-H activations, followed by the N-containing groups<sup>[13]</sup> and then the corresponding second row substituents<sup>[14]</sup>. It is not surprising that the experimental yields of DHR might be highly dependent on the nature of directing groups

on both arenes and alkenes.

In 2012, Zhang and co-workers<sup>[3e]</sup> reported an efficient DHR between benzylmethylsulfide (**1a**) and methyl acrylate (**2**) by the catalytic Pd(OAc)<sub>2</sub> (see Scheme 1). Interestingly, no desired coupling-product was detected if the substrate methylthio (-SCH<sub>3</sub>) was replaced by a methoxyl (-OCH<sub>3</sub>) under the identical reaction conditions, in contrast to many precedents of directed C-H functionalizations by the aid of O-containing substituents. A related hydroarylation of methyl acrylate reported by Jun and co-workers<sup>[13f]</sup> disclosed that acetylbenzene was an inert aromatic substrate under the catalysis of Rh(PPh<sub>3</sub>)<sub>3</sub>Cl; nevertheless, using the corresponding arylketimine as a substrate afforded good yields under the same reaction conditions. These examples indicated that S- or N-centre groups should be more competent for directing the couplings with methyl acrylate than the O-centre counterparts.

**Scheme 1.** Directing Group Dependent Arene-Alkene Cross-coupling Reactions, Simulated in this Work by DFT Calculations.



Screening compatible alkene partners under certain DHR conditions has been much discussed in a large number of papers<sup>[2]</sup>. In general, electronically biased alkenes, such as  $\alpha,\beta$ -unsaturated ketones and esters, are more active toward migratory insertion reactions than non-functionalized alkenes<sup>[15]</sup>. As a prototype of activated alkenes, styrene<sup>[8b,16]</sup> was able to couple with a wide range of arenes in good yields. Recently, Ellman and co-workers<sup>[15e]</sup> reported that 1-hexene could become a good coupling-partner of aryl O-methyl oximes when using the catalytic [Cp\**Rh*Cl<sub>2</sub>]<sub>2</sub> with the additive of AgSbF<sub>6</sub>.

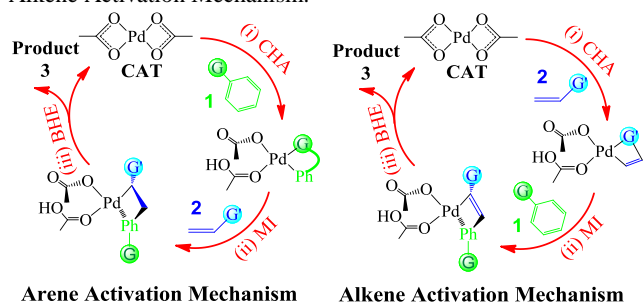
Considering the green-chemistry advantages of DHRs and their

importance to the C-C bond-formation, development of theoretical understanding on how these reaction conditions affect experimental yields is of great value for organic chemists. Among all the experimental variables, directing group effect is the main topic of this study, and therefore, the density functional theory (DFT) method will be conducted to systematically explore the role of directing groups on both arenes and alkenes.

## Results and Discussion

The DHR reactions between arenes and alkenes were traditionally decomposed into three successive processes<sup>[2]</sup>, namely, C-H activation (CHA), migration insertion (MI), and  $\beta$ -H elimination (BHE) and recovery of catalyst (RC). For the reaction of **1** (**1a** or **1b**) with **2** (see Scheme 1), however, two competing reaction mechanisms are proposed in this work, considering both **1** and **2** could undergo CHA transformation with Pd(OAc)<sub>2</sub> *via* five-member cyclopalladation. If the CHA of arene **1** takes place first, alkene **2** needs to serve as a coupling partner participating in the following MI reaction. Since this reaction pathway is initiated by activating an aromatic C-H bond, it is referred to herein as arene activation mechanism (see the left circle in Scheme 2). Alternatively, if the CHA of alkene **2** is the first process, arene **1** must act the role of coupling partner in the subsequent step, and this reaction channel is correspondingly denoted as alkene activation mechanism (see the right circle in Scheme 2). The following subsections will disclose how the nature of directing groups determines the dominance of these two reaction mechanisms and influences the yields of cross-coupling products.

**Scheme 2.** General Processes for the Dehydrogenative Heck Coupling between an Arene (**1**) and an Alkene (**2**) Simulated in this Work by DFT Calculations: Arene Activation Mechanism vs. Alkene Activation Mechanism.



### Arene Activation Mechanism

For the DHR of **1** (**1a** or **1b**) with **2**, the common arene activation mechanism was first simulated, and the entire reaction pathway is schematically depicted in Figure 1 along with the atomic numbering used. In the following discussion, the notation X = a (G = S) is used for **1a**+**2** and that of X = b (G = O) is used for **1b**+**2**. It is easily realized that the substrate-catalyst encounter, occurring in a one-step ligand exchange, is unambiguously initiated by the substrate heteroatom, passing through a five-coordinate transition state (**TS-1X**) with two incipient bonds of Pd-G and Pd-O1. As the approach of the heteroatom and the departure of the O1-arm, a square complex intermediate (**INT-1X**) would be formed in the manner of changing one of the two  $\kappa^2$ -acetate ligands to the  $\kappa^1$ -ligated structure. It was generally

believed that such coordination between **1** and Pd(OAc)<sub>2</sub> would result in the enhancement of chemical reactivity and/or selectivity at the substrate active centre, according to the complex-induced proximity effect (CIPE)<sup>[11]</sup> in C-H activation chemistry.

However, the aromatic C5-H bond, *ortho* to the branch chain, is still unavailable for any interaction with the palladium centre in **INT-1X** (~4.0 Å for C5...Pd distance), negating the potential for C-H activation directly from such an intermediate. In this respect, another four-coordinate complex with a loose Pd...C5 interaction (2.4 ~ 2.5 Å) has been located and characterized as the precursor of C-H cleavage step; the geometric structure of this species is not shown in Figure 1 for simplicity sake.

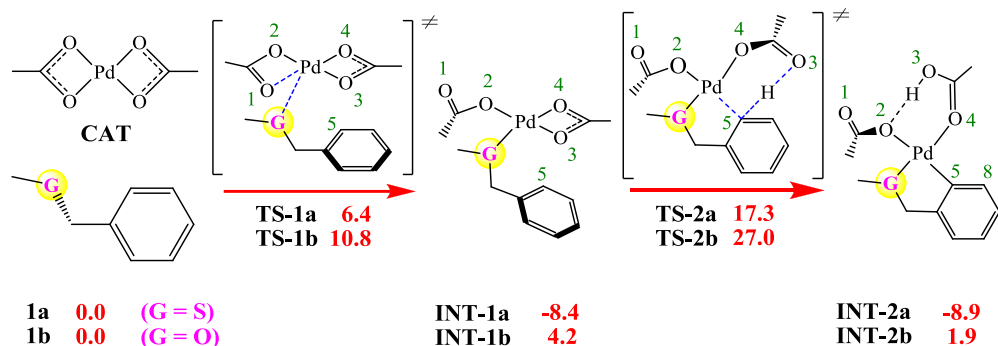
The typical hydrogen-transfer transition state (**TS-2X**), a six-member ring structure, has been located, in which the proton-abstraction is induced by the *cis*-acetate O3-atom, accompanied by formation of a Pd-C5  $\sigma$ -bond (2.43 Å in **TS-2a** or 2.17 Å in **TS-2b**). The H-atom in motion is nearly at the midpoint of O3...C5 line, e.g., the distances of H...O3 and H...C5 in **TS-2a** are 1.35 and 1.34 Å, respectively. IRC calculations confirmed that a counter-clockwise rotation along Pd-O4 bond leads to formation of an intramolecular H-bond (O3-H...O2) in the reaction successor (**INT-2X**), if the geometry of **TS-2X** is relaxed along the forward direction.

The intermediate **INT-2X** is of four-coordinate planar structure, allowing the olefinic partner, methyl acrylate (**2**), to participate in the MI process from the top of the coordination plane *via* **TS-3X** transition state. MI reactions can be formally considered as a kind of concerted [ $2\sigma + 2\pi$ ] cycloaddition reactions involving a metal-nonmetal  $\sigma$ -bonding and a carbon-carbon or carbon-heteroatom  $\pi$ -bonding, e.g., Pd-C5  $\sigma$ -bond and olefinic  $\pi$ -bond for the present study. Generally speaking, cycloadditions involving four  $\pi$ -electrons are traditionally believed to be kinetically forbidden under the thermochemical conditions for orbital symmetry consideration. However, the engagement of the low-lying (n-1)*d*-orbitals at the metallic centre could make the involved "orbital pairs" symmetrically matched,<sup>[17]</sup> facilitating the related chemical bond reorganizations. The MI transition state herein (**TS-3X**) is a typical four-member ring structure, showing formation of two  $\sigma$ -bonds of Pd-C7 and C5-C6 concomitant with cleavage of a Pd-C5  $\sigma$ -bond and a C6-C7  $\pi$ -bond. All incipient bond lengths are consistent with our chemical intuition, for example, the bond lengths of Pd-C5, Pd-C7, C5-C6 and C6-C7 in **TS-3a** are calculated to be 2.13, 2.14, 2.03 and 1.44 Å, respectively. Some secondary structural changes can be noticed during the relaxation of **TS-3X** along the forward reaction route, including the departure of G-group and the re-coordination of O4-arm. Besides these, the aromatic ring was observed to stick on the metallic centre through Pd- $\pi$  interaction using its one edge (C5-C8), probably due to the four-coordinate propensity for Pd<sup>II</sup>-centre.

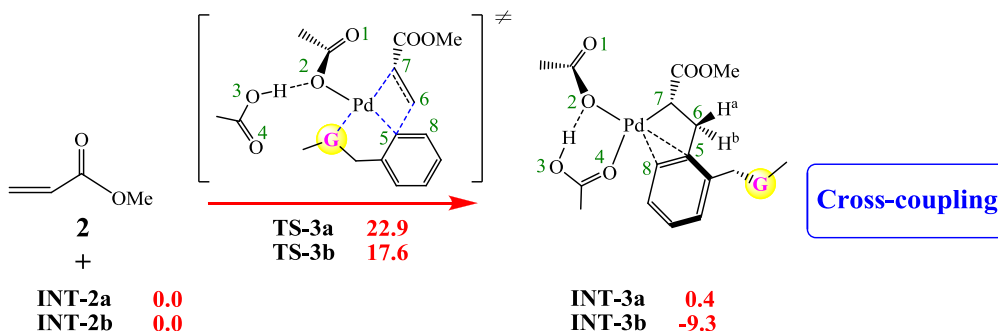
To form the coupling product (**3a** or **3b**), the bonding between C6 and C7 must be recovered to be a double-bond, that is, one of the two H-atoms on C6 needs to be eliminated and the Pd-C7  $\sigma$ -bond will be simultaneously destroyed, which is a typical  $\beta$ -H elimination (BHE) process. There are two potential channels for BHE depending on the selection of removing H<sup>a</sup> or H<sup>b</sup> from **INT-3X**, in which the stereoselectivity related to the geometric isomerism of the C6-C7 double-bond is determined by either a *cis* or *trans* olefinic group in **3**. In fact, a rotation about the C6-C7

bond can bring one of the two H-atoms proximal to the central palladium, which is favourable for the BHE step. The clockwise rotation by *ca.* 60°, as shown in Figure 1, affords **INT-4X** with the *trans* arrangement of the phenyl and the ester group relative to the C6-C7 bond, in which the H<sup>b</sup> atom shifts from C6 to palladium centre and the Pd-C7  $\sigma$ -bond becomes a loose Pd- $\pi$  interaction *via* a four-member ring transition state (**TS-5X**). The

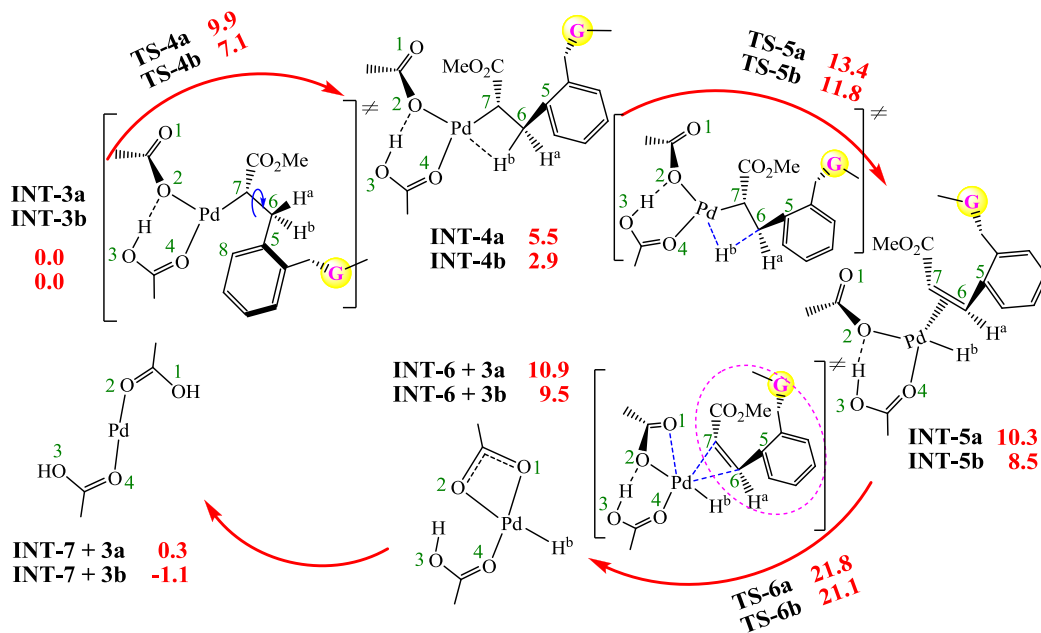
alternative counter-clockwise C6-C7 rotation will result in the elimination of H<sup>a</sup> and thus yield the unfavourable *cis*-**3** *via* a similar BHE transition state. Our calculation results confirmed that the formation of *trans*-**3** is kinetically more favourable than that of *cis*-**3** (see data given in the Supplementary Information). Therefore, *trans*-**3** is denoted as **3** for convenience afterwards.



### A. C-H Activation of 1 with Catalyst



### B. Migratory Insertion of INT-2a or INT-2b with 2



### C. $\beta$ -H Elimination & Recycling of Catalyst

**Figure 1.** Arene activation mechanism of **1** (**1a** or **1b**) with **2** simulated by DFT calculations. The values beside structures show the variations of Gibbs free-energy (in red, kcal/mol) along reaction coordinates.



Cite this: DOI: 10.1039/c0xx00000x

www.rsc.org/xxxxxx

## ARTICLE TYPE

Up to now, the final product **3** is still stick on the central palladium through Pd- $\pi$  bonding due to the four-coordinate preference of Pd<sup>II</sup>-complexes. However, an intramolecular ligand substitution, mediated by the acetate O1-atom, could get rid of product **3** and recovers itself to the  $\kappa^2$ -acetate structure, leading to an intermediate of **INT-6**. And then H<sup>b</sup> can easily shift from the metal centre to the O1-arm of the  $\kappa^2$ -acetate and simultaneously, the Pd-O1 coordination bond will be cleaved to afford a two-coordinate complex (**INT-7**) with two ligands of acetic acid in linear arrangement. The step of **INT-6**→**INT-7** changes the acidity of H<sup>b</sup>, since H<sup>b</sup> is involved in the polar O-H bond in **INT-7**. Upon this hydrogen-transfer, the formal oxidation state of the central palladium is reduced from +2 to 0 (Pd<sup>II</sup>→Pd<sup>0</sup>). The recovery of catalyst Pd(OAc)<sub>2</sub>, using two molecules of oxidant AgOAc, is a complicated redox process, which was simulated with Ag<sub>2</sub> cluster in our previous work.<sup>[18]</sup>

The kinetic and thermodynamic characterization of the overall reaction is reported herein based on the relative solution free-energies calculated at the B3LYP-IDSCRF/DZVP level of theory (see the red values in Figure 1), while those generated with other methods are available in the Supplementary Information for saving space.

It can be observed that the free-energy change of the first step, the substrate-catalyst combination, is -8.4 kcal/mol for **1a** and +4.2 kcal/mol for **1b**, meaning that the formation of **INT-1a** is a spontaneous process whereas that of **INT-1b** is disfavoured in a chemical equilibrium perspective. If the subsequent processes (CHA and MI) take place readily and will lower the free energies, the cross-coupling of **1b+2** might be driven to proceed further. According to the steady-state approximation,<sup>[19]</sup> the rate-controlling barrier of C-H activation of **1a** is 25.7 kcal/mol determined by the free-energy difference between **INT-1a** and **TS-2a**, while that of **1b** increases to 27.0 kcal/mol; the calculated half-life time at 373K is 2.5 min (**1a**) or 14 min (**1b**). The overall reaction free-energy for the transformation of Pd(OAc)<sub>2</sub> + **1** → **INT-2X** is estimated to be -8.9 (**1a**) or +1.9 (**1b**) kcal/mol, favouring **1a** as well. Note that all of the stationary points on the CHA pathway are 9 ~ 12 kcal/mol more stable for the S-system with respect to the O-system, which is parallel with our calculated bond dissociation energies of Pd-G that Pd-S coordination bond is *ca.* 10 kcal/mol inherently more stronger than Pd-O.

In contrast to the CHA process, the next MI process from **INT-2X** to **INT-3X** discriminates the O-system against the S-system both kinetically and thermodynamically. Specifically, the free energy barrier of MI is 22.9 kcal/mol for **TS-3a** and 17.6 kcal/mol for **TS-3b**, and formation of **INT-3b** from **INT-2b** will release free energy of 9.3 kcal/mol comparing with the energetically neutral reaction of **INT-2a**→**INT-3a**, because this MI step involves cleavage of the Pd-G bond formed previously. The following transformation is the multi-step BHE process from **INT-3X** to **INT-7**, which should proceed easily without high-lying transition state. As for the Pd<sup>0</sup>→Pd<sup>II</sup> reoxidation, the

complete simulation with DFT method is too difficult and complicated. Our molecular modelling based on the silver cluster model led to the results that this reoxidation process is both dynamically and thermodynamically available, since the calculated free-energy barrier and reaction free-energy are 20.8 and -11.2 kcal/mol; details are available in the Supplementary Information.

Based on these results, it can be stated that the reaction of **1b+2** should proceed more slowly than that of **1a+2**, but one cannot explain the complete inertness of **1b+2** experimentally observed. We must explore the alternative alkene activation mechanism to fully understand the directing group effect occurring in these DHRs in the following section.

### Alkene Activation Mechanism

In order to differentiate the activity between **1a** and **1b** toward the same alkene **2**, the alkene activation mechanism for the same cross-coupling has been comparatively explored, as illustrated in Figure 2. Such investigation might provide a most probable clue to rationalize the directing group effect occurring in the DHRs.

Figure 2 shows that this reaction pathway starts from the CHA of **2**, which should be preceded by a pre-coordination between **2** and catalyst. The carbonyl oxygen in complex **INT2-1** facilitates the cleavage of a terminal C-H bond of **2**, leading to the five-member cyclopalladation product **INT2-2**. The hydrogen transfer transition state (**TS2-2**) is feathered by a six-member ring frame, similar to **TS-2X**, with the distances of O3...H and C5...H being 1.39 and 1.33 Å, respectively.

In order to form the cross-coupling product **3**, **1** must react with **INT2-2** via the MI pathway to construct a C-C bond between **1** and **2**. The four-centre transition state **TS2-3X** has been located, which involves the insertion of one side of the benzene ring into the Pd-C5  $\sigma$ -bond, generating an intermediate **INT2-3X** with a cyclohexadiene fragment. Afterwards, **INT2-3X** can aromatize to **3** concomitant with recovery of Pd(OAc)<sub>2</sub> through BHE and RC processes.

One can notice from Figure 2 that the coordination of **2** is nearly free-energy neutral (+1.0 kcal/mol), which lies between those of **1a** and **1b**, meaning that Pd(OAc)<sub>2</sub>+**2** and **INT2-1** are almost thermodynamically unbiased. The free-energy barrier of **TS2-2** is calculated to be 28.8 kcal/mol that is higher than **TS-2a** but close to **TS-2b**. The intermediate product **INT2-2** is slightly stabilized by *ca.* 1.5 kcal/mol, indicating this process is accessible both kinetically and thermodynamically. The MI reaction of **1** with **INT2-2**, however, becomes very challenging with the free-energy barrier of 31.5 (**1a**) or 33.3 (**1b**) kcal/mol. Furthermore, the generated intermediate **INT2-3X** is highly unstable (+21.2 ~ +23.3 kcal/mol), implying this reaction should be prohibited at 373 K. It is mainly because addition of the Pd-C5  $\sigma$ -bond onto a benzene carbon-carbon edge results in loss of aromaticity. Therefore, it can be concluded that the cross-coupling product cannot be formed through alkene activation mechanism.

The destiny of the possible  $\sigma$ -vinylpalladium(II) complex has

also been addressed herein, and **INT2-2** could easily react with a second molecule of **2** to give the homo-coupling side-product *via* **TS2-hom**, as homo-couplings are the common side-reactions for transition-metal catalysed C-C cross-coupling reactions.<sup>[11]</sup>

5 In brief, once the reaction system enters the “alkene activation  
10

circle”, formation of cross-coupling products seems to be precluded due to the inertness of **INT2-2** with **1**. In next section, we will discuss how the nature of directing groups governs the competition of different mechanisms.

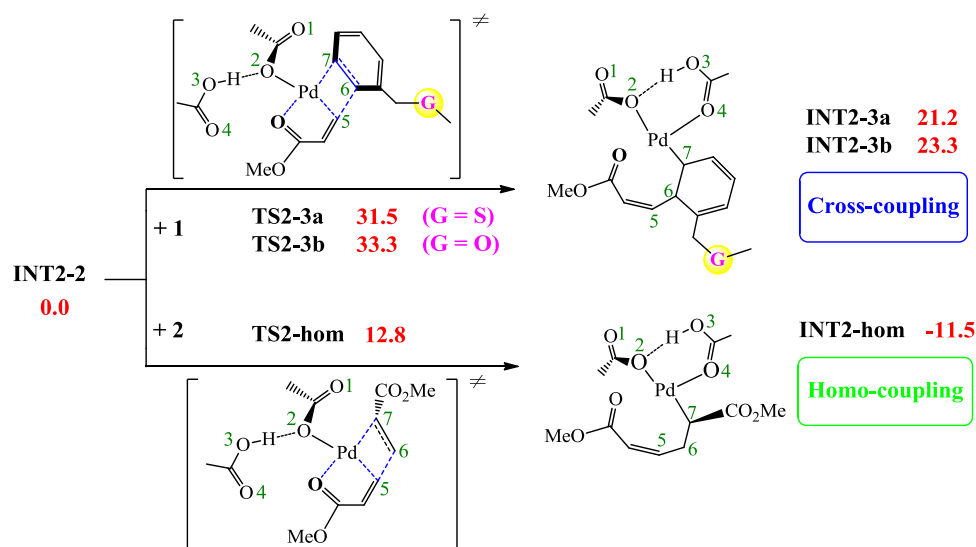
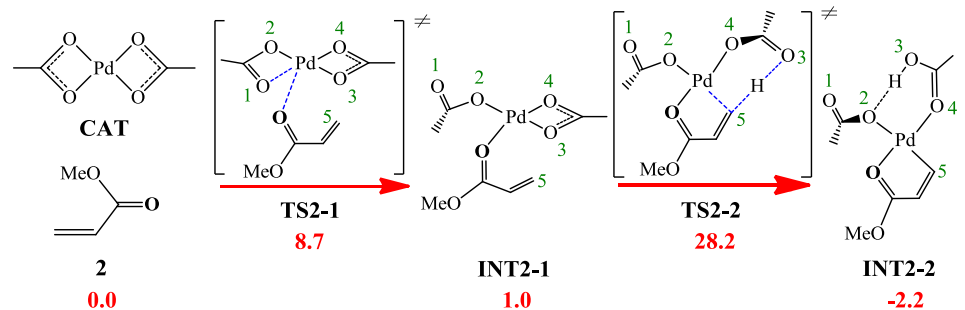


**Figure 2.** Alkene activation mechanism for the cross-coupling of **2** with **1** (**1a** or **1b**) and the homo-coupling of **2**. The values beside structures show the variations of Gibbs free-energy (in red, kcal/mol) calculated at the B3LYP-IDSCRF/DZVP level of theory.

### Directing Group Effect—Arene Activation vs. Alkene Activation

15 Figure 3 depicts the calculated free-energy profiles for the DHRs of **1a+2** and **1b+2**, containing both arene activation mechanism and alkene activation mechanism. For the **1a+2** cross-coupling (blue curve vs. green curve), the arene activation mechanism is  
20 absolutely more advantageous than its opponent (alkene activation mechanism). It is easily noticed that coordination of **1a** with catalyst should predominate over that of **2** in the reactant mixture, since the former process releases free energy of 8.4 kcal/mol and the latter one is free-energy unbiased. And  
25 kinetically, the free-energy barrier of this step is also lower for the coordination of **1a** than that of **2**. Besides, most stationary points on the blue curve are more stable than those on the green curve, ensuring this reaction should always proceed *via* the favourable arene activation mechanism.

30 For the **1b+2** cross-coupling (red curve vs. green curve), however, coordination of **1b** with catalyst is endothermic by 4.2 kcal/mol, which seems unfavourable comparing with that of **2**. Parallely, the transition state **TS-1b** is 2.1 kcal/mol less stable than the transition state **TS2-1**. Owing to the kinetic and  
35 thermodynamic similarities between the C-H activations of **1b+Pd(OAc)<sub>2</sub>** and **2+Pd(OAc)<sub>2</sub>**, the relative coordination ability of **1b** and **2** with catalyst might determine their reaction sequences in the entire catalytic cycle. Since the smaller **2**  
40 molecule is more inclined to combine with catalyst with respect to the larger **1b**, **INT2-1**, rather than **INT-1b**, should predominate the equilibrium concentration. Afterwards, the overall reaction will follow the alkene activation mechanism, whereas formation of cross-coupling product is hindered by an unfeasible MI  
45 readily react with a second molecule of **2** to form the homo-

coupling side-product involving a free-energy barrier of only 12.8 kcal/mol.

In brief, the stronger coordination capability of arenes relative to alkenes should be one of the aspects propitious to the efficiency of DHRs. A DHR might switch to alkene activation mechanism, if the aromatic substrate bears a relatively poor directing group, leading to a  $\sigma$ -vinylpalladium(II) intermediate,

which is inaccessible for formation of the desired arylalkenes.

The main reason of the good performance for the **1a**+**2** cross-coupling lies in the better coordination ability of S-atom with comparison to O-atom. Electronic topology analyses based on Bader's atoms-in-molecules theory were performed to understand the origin of bonding reinforcement of Pd-S relative to Pd-O.

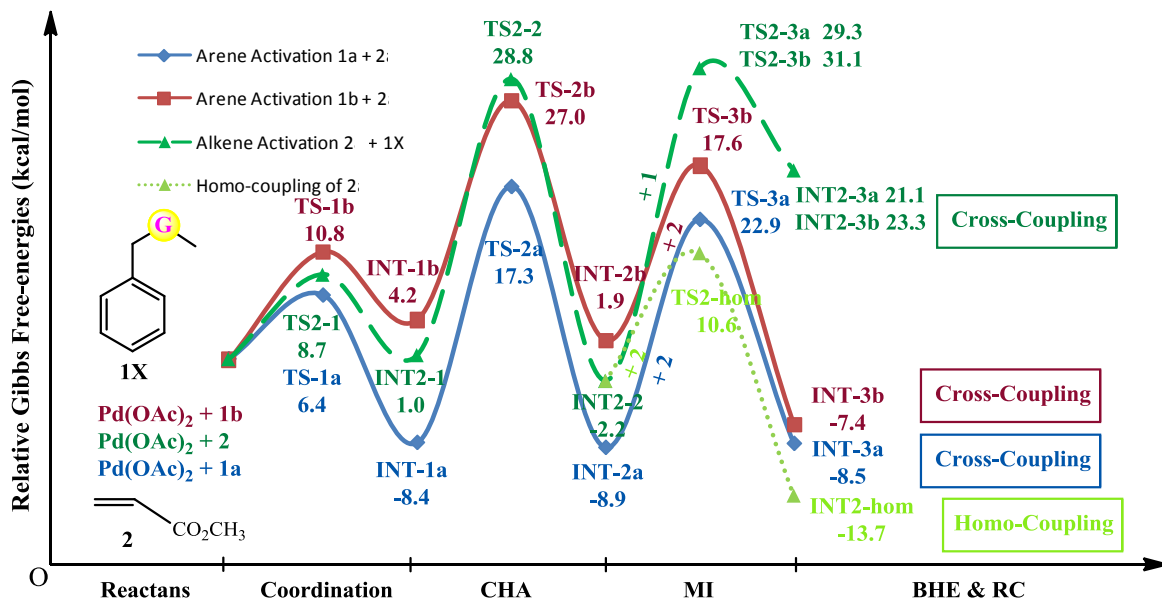


**Figure 3.** Free-energy (in kcal/mol) profiles for the reactions of **1a**+**2** and **1b**+**2**, calculated at the B3LYP-IDSCRF/DZVP level of theory. Arene activation mechanism and alkene activation mechanism are comparatively shown, where BHE and RC processes are omitted for simplicity sake.

Figure 4 shows the 2-D isodensity surface plots of the Laplacian of electron densities ( $\nabla^2\rho$ ) for the complexes of Pd(OAc)<sub>2</sub>+**1a** (left), Pd(OAc)<sub>2</sub>+**1b** (middle) and Pd(OAc)<sub>2</sub>+**2** (right), from which one can observe that the electron density ( $\rho_b$ ) at the Pd-S bond critical point (bcp) (0.097 a.u.) is substantially larger than those at the corresponding Pd-O bcps (0.067 and 0.071 a.u.), meaning Pd-S coordination bond is inherently stronger than Pd-O. Such results indicate that the DHR between a sulfur-substituted arene and an oxygen-substituted alkene should surely follow the favorable arene activation mechanism. The difference of  $\rho_b$  between the coordination Pd-O bonds of Pd(OAc)<sub>2</sub>+**1b** and Pd(OAc)<sub>2</sub>+**2** shows that the carbonyl oxygen in **2** is coordinatively better than the ether oxygen in **1b**. And

interestingly, the directions of these Pd-L bond paths are parallel with the calculated bonding free-energies of these three complexes. Notably, the Pd-S bond path is starting from the maxima of valence electron density on the S-atom to the depletion region of Pd atom, like a 'key-lock' stronger interaction; the direction of the Pd-O bond path in the middle complex obviously deviates from the maxima of valence electron density on the O-atom (weaker interaction); only trivial deviation can be observed in the Pd-O bond path of the right complex (slightly weaker interaction). It is, therefore, worth noticing that the relative coordination capability of arenes and alkenes is one of the most important factors determining the reaction mechanism and reaction energy profiles.

Cite this: DOI: 10.1039/c0xx00000x

www.rsc.org/xxxxxx

ARTICLE TYPE

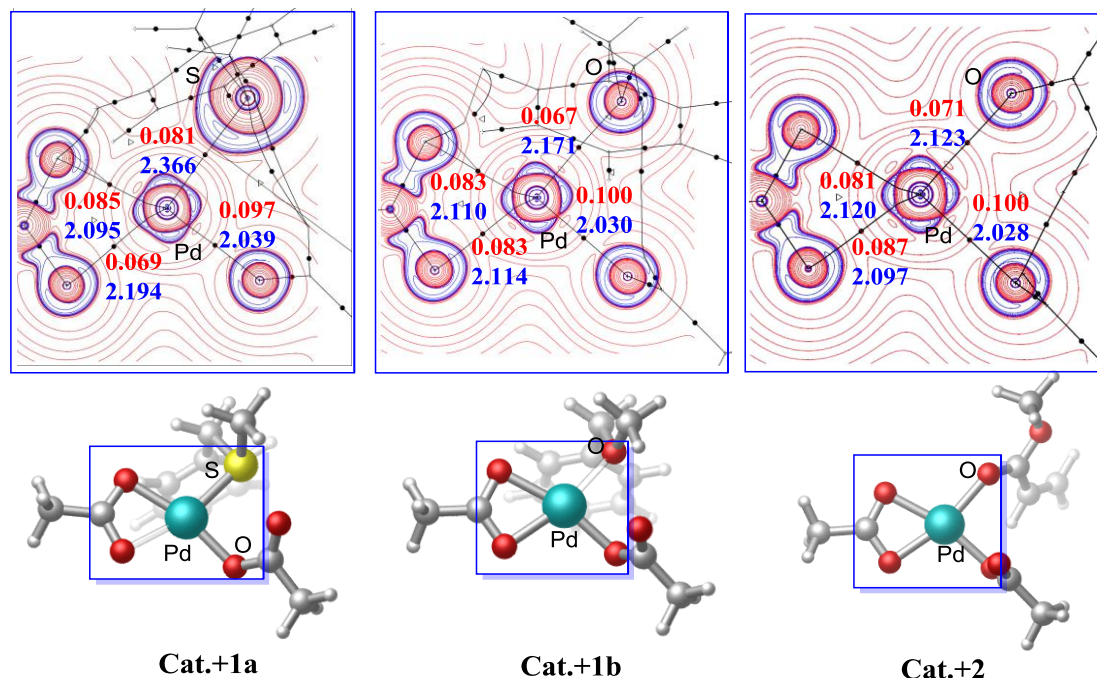


**Figure 4.** ORTEP plot of the complexes formed between catalyst and different reactants (**1a**, **1b** and **2**). Depiction of the “onion layer” 2-D isodensity surfaces were provided from the Laplacian of electron densities ( $\nabla^2\rho$ ) in the selected plane, with the bond lengths (Å), bond paths, electron densities ( $\rho_b$  in a.u.) and bond critical points are shown in blue text, solid black line, red text and small black dot, respectively.

#### More Directing Groups and Their Reactivities

In order to account for a wider range of directing groups, some simple molecules were designed as the models of aromatic substrates used in the DHRs (see Table 1). These model molecules can be classified into two groups:  $sp^3$ -X and  $sp^2$ -X, which are for the aromatic compounds bearing  $sp^3$ -hybrid and  $sp^2$ -hybrid coordination centres, respectively. Since the relative coordination ability of arenes and alkenes might govern the reaction mechanism and thus influence the reaction yields, it is necessary to collect the data in Table 1 for the bonding free-energies of Pd(OAc)<sub>2</sub> with each of these compounds, calculated at the B3LYP-IDSCRF/DZVP level of theory, which might guide the experimentalists for references.

The validity of these theoretical data can be tested by comparing with the related experimental evidence reported in the literature. Our calculations first indicated the greatest directing tendency of  $-P(CH_3)_2$  group among all the substituents in Table 1, with the coordination free-energy of  $sp^3$ -P being  $-23.2$  kcal/mol. In fact, Rh-catalysed *ortho* C-H activations on phosphine ligands have been previously reported by different research groups<sup>[14a-14c]</sup>, where a phosphorus-incorporating cyclometalated species was accepted as a shared intermediate. Only second to  $sp^3$ -P, thioether  $sp^3$ -S bears an excellent directing group  $-SCH_3$  whose coordination free-energy is calculated to be  $-8.4$  kcal/mol, consistent with the successful DHR of  $sp^3$ -S with methyl acrylate reported by Zhang and co-workers<sup>[3e]</sup>. As an analogue of  $-P(CH_3)_3$ , the group  $-N(CH_3)_2$  also exhibits commendable directing

property, similar to the group  $-SCH_3$ . In experiment, independent works conducted by Shi and Yu disclosed that both N,N-dimethylbenzylamine<sup>[20]</sup> and mono-protected phenethylamine<sup>[21]</sup> could couple with some acrylates effectively under their respective optimal conditions. These combined theoretical and experimental findings obviously support that N-atom serves as a better directing centre than O-atom, since the calculated bonding free-energy of  $sp^3$ -O with Pd(OAc)<sub>2</sub> is *ca.*+4.2 kcal/mol, substantially more positive than that of  $sp^3$ -N. Despite a large number of other types of C-H activation transformations directed by O-containing groups have been available in the literature<sup>[12]</sup>, the DHR with acrylates using an aromatic ether as a substrate was not reported yet, probably due to the existence of a relatively better directing group in the methyl acrylate (see the last entry of Table 1). Organic halides (e.g., PhCH<sub>2</sub>Cl and PhCH<sub>2</sub>F) seem not to be effective ligands of the Pd-centre due to the large positive values of bonding free-energy (see the entries for  $sp^3$ -F and  $sp^3$ -Cl); consistently, there has been no direct experimental evidence supporting the existence of any cyclometalated species containing a halogen, till now.

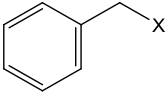
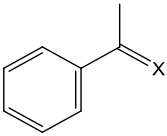
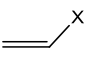
It can be observed from Table 1 that compounds with the  $sp^2$ -hybrid X have similar reactivities as those of  $sp^3$ -hybrid X, but the  $sp^2$ -hybrid atomic centre, in general, shows greater coordination inclination than the  $sp^3$ -hybrid counterparts for O- and N-atoms. Conversely, the S- and P-substituents display the reverse effect, as shown from the data of the coordination free-energies in Table 1, thus resulting in an overall order of P > N >



S > O within  $sp^2$ -X systems. AIM analyses have been performed to study the electron density distributions of these complexes, and the electron density values at the bcps are parallel with the calculated bonding free-energies (see data given in the Supplementary Information). The bond-lengths (see  $d_{Pd-X}$  in Table 1) of these Pd-X coordination bonds are also in good agreement with the calculated bonding free-energies.

Judging from the data in Table 1, arylimine  $sp^2$ -N has a stronger propensity for coordination with Pd<sup>II</sup>-centre than the corresponding arylketone ( $sp^2$ -O), and thus, it is not difficult to understand that  $sp^2$ -O system could only couple with simple

**Table 1.** Relative bonding free-energies ( $\Delta G$  in kcal/mol) and activation free-energies ( $\Delta G^\ddagger$  in kcal/mol) of Pd(OAc)<sub>2</sub> with different functionalized reactants, calculated Pd-X bond-lengths ( $d_{Pd-X}$  in Å), predicted reaction pathway of DHR with methyl acrylate (Pred. path) and the related experimental evidence in the literature (Expt. obs.).

Structures	X	Abbr.	$\Delta G$	$\Delta G^\ddagger$	$d_{Pd-X}$	Pred. path	Expt. obs.
	P(CH <sub>3</sub> ) <sub>2</sub>	$sp^3$ -P	-23.2	-	2.294	Arene act.	-
	SCH <sub>3</sub>	$sp^3$ -S	-8.4	6.4	2.366	Arene act.	r <sup>[3e]</sup>
	N(CH <sub>3</sub> ) <sub>2</sub>	$sp^3$ -N	-7.6	7.6	2.135	Arene act.	r <sup>[20,21]</sup>
	OCH <sub>3</sub>	$sp^3$ -O	+4.2	10.8	2.171	Alkene act.	nr <sup>[3e]</sup>
	Cl	$sp^3$ -Cl	+6.6	10.2	2.472	Alkene act.	nr
	F	$sp^3$ -F	+9.7	10.0	2.250	Alkene act.	nr
	PCH <sub>3</sub>	$sp^2$ -P	-12.7	6.5	2.297	Arene act.	-
	N	$sp^2$ -N	-10.3	6.9	2.075	Arene act.	r <sup>[13f-13h]</sup>
	S	$sp^2$ -S	-6.4	8.2	2.344	Arene act.	-
	O	$sp^2$ -O	+2.8	9.6	2.116	Boundary	r <sup>[8,23]</sup> /nr <sup>[13f,23b]</sup>
	COOCH <sub>3</sub>		+1.0	8.7	2.123		

As the centrality of carbonyl in organic chemistry<sup>[22]</sup>, carboxylic acid derivatives are very common synthetic raw materials. In fact, the directing capability of carbonyl oxygen in  $sp^2$ -O is only slightly weaker than that in methyl acrylate, perhaps implying a surmountable hindrance occurring in the DHRs of aromatic carbonyls with acrylates. Therefore, these DHRs might show boundary behaviour and could be improved by optimization of other reaction conditions, such as peripheric modulation on reaction centre, ligand field of catalyst and additives. Experimentally, the DHRs of phenylacetic acids with acrylates were performed well in the presence of some chiral amino acids as auxiliary ligands<sup>[8]</sup>. Although acetylbenzene could not couple with acrylates in the hydroarylation reactions<sup>[13f]</sup>, N-phenylacetamides could couple with a wide range of alkene partners favourably.<sup>[23]</sup> Our calculations also show that modification of the reactants of the  $sp^2$ -O system might result in the change of reaction mechanisms, since the bonding free-energies of the different carbonyl compounds used in the cross-couplings are close with one another. For example, N-(p-

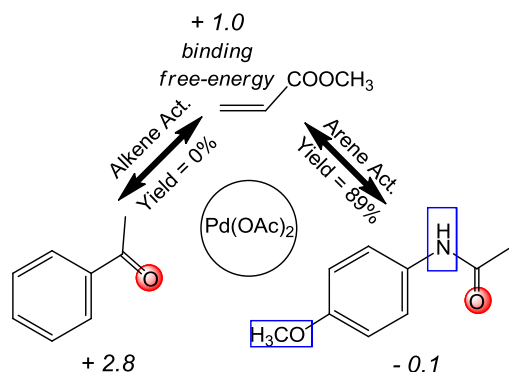
alkenes (e.g., 1-hexene),<sup>[13f]</sup> whereas the corresponding arylketimine is able to couple with both simple and functionalized alkenes (e.g., acrylates) in moderate to good yields<sup>[13f]</sup>. These are attributed to the medium coordination capability of  $sp^2$ -O lying between those of 1-hexene and acrylates, resulting in the switch of reaction mechanism from arene activation for  $sp^2$ -O with 1-hexene to alkene activation for  $sp^2$ -O with acrylates. In contrast,  $sp^2$ -N has a better coordination N-centre with respect to methyl acrylate and 1-hexene, achieving efficient cross-coupling with each of them.

methoxyphenyl)acetamide could combine with Pd(OAc)<sub>2</sub> with releasing the free-energy of 0.1 kcal/mol, slightly more favorable than that of methyl acrylate with Pd(OAc)<sub>2</sub>, which could avoid the C-H activation on the methyl acrylate (see Scheme 3).

Since thiocarbonyl compounds were not as prevalent as the corresponding carbonyl compounds in organic synthesis, direct evidence of thiocarbonyl-mediated DHR can hardly be found in the literature. Based on our calculations, however, thioetone ( $sp^2$ -S) was predicted to be adequate for the directed DHR with the bonding free-energy of -6.4 kcal/mol. Phosphaalkene ( $sp^2$ -P), a less common organic reactant, was modelled for comparative purpose, which theoretically exhibited the best directing property and was predicted to be a good aromatic substrate for DHRs.

It is noteworthy that the thermodynamic trend ( $\Delta G$ ) and the kinetic trend ( $\Delta G^\ddagger$ ) of these coordination reactions, reflected in Table 1, are consistent with each other, since a larger free-energy release accompanies a lower free-energy barrier for a given directing group system.

**Scheme 3.** The Substitution Dependent Arene-Alkene Cross-coupling Reactions, along with the Calculated Bonding Free-energies (kcal/mol), Predicted Reaction Mechanisms and Experimental Yields.



In brief, the relative bonding free-energies of arenes and alkenes with catalyst, as list in Table 1, provided a theoretical guidance for screening compatible reactants in the Pd-catalysed DHRs. The investigation on different substrates and catalysts are still underway in our group.

## Conclusions

B3LYP-IDSCRF/DZVP calculations have been performed to characterize the plausible mechanism and directing group effect occurring in the Pd-catalysed DHRs. The following conclusions have been reached:

- (1) Two probable reaction routes, namely, arene activation mechanism and alkene activation mechanism, have been found, in which the latter would favour the homo-coupling of alkenes.
- (2) The nature of directing groups on arenes and alkenes should mainly determine the competition between these two possible reaction routes. Better directing groups on arenes with respect to alkenes could ensure the favourable arene activation mechanism; otherwise, the catalysed reaction might switch to the alkene activation mechanism, resulting in the reduction of desired product yields.
- (3) The coordination abilities of different directing groups are  $P > S > N > O$  for the  $sp^3$ -X series, while they are  $P > N > S > O$  for the  $sp^2$ -X systems.

## Experimental

All geometric parameters for reactants, products, complexes, intermediates and transition states have been optimised and verified with the B3LYP method as implemented in Gaussian 09<sup>[24]</sup>, employing the standard double- $\zeta$  valence polarized (DZVP) all-electron basis set<sup>[25]</sup> for all atoms. The polarizable continuum model (PCM)<sup>[26]</sup> was used with DCE as solvent, while our IDSCRF radii<sup>[27]</sup> has been chosen as the atomic radii to define the molecular cavity, denoted B3LYP-IDSCRF in this work. All resultant stationary points were subsequently characterised by frequency analyses, from which the zero-point energies were obtained for calculating the total energies, in addition to ensure that the obtained structures resided at minima or first-order saddle points on their potential energy hypersurfaces. Intrinsic reaction coordinate (IRC)<sup>[28]</sup> computations with the Hessian-based predictor-corrector integrator (HPC)<sup>[28b,28c]</sup> were used to trace

some selected reaction paths to confirm the optimised saddle point as being on the correct reaction pathway.

Solution translational entropy has been calculated with our THERMO program<sup>[29]</sup>, in order to get reasonable free-energy barriers for solution reactions. To account for the basis set effect, single point calculations have been performed using a larger and mixed basis set (BS1), where the 6-311+G(d,p) basis set is used for non-metal elements and the DZVP basis set is used for transition-metal elements. Besides, all the stationary points have been re-optimised at the M062x<sup>[30]</sup>-IDSCRF/DZVP level of theory, and then single point calculations have been performed at the M062x-IDSCRF/BS1 level of theory.

The electronic structures of selected structures were analysed by Bader's atoms-in-molecules (AIM)<sup>[31]</sup> analyses, to quantitatively characterize the topological properties of the electron density distributions. Analyses were carried out on the wave functions generated with the B3LYP-IDSCRF/DZVP method on the geometry-optimized structures. All molecular graphs and 2-dimensional Laplacian reported in this article have been performed with the AIM98PC<sup>[32]</sup> program package, a modified version of the AIMPAC program.<sup>[33]</sup>

## Acknowledgements

This work was supported by the National Nature Science Foundation of China (21373030).

## Notes and references

- <sup>70</sup> <sup>a</sup>College of Chemistry, Beijing Normal University, Beijing 100875, China. Fax: 086-10-58802705; Tel: 086-10-58805422; E-mail: dcfang@bnu.edu.cn
- <sup>71</sup> † Electronic Supplementary Information (ESI) available: [The optimized geometric parameters, frequencies, energies and free energies are available in this ESI]. See DOI: 10.1039/b000000x/
- 1 M. M. Heravi, E. Hashemi and N. Ghobadi, *Curr. Org. Chem.*, 2013, **17**, 2192; D. Mc Cartney and P. J. Guiry, *Chem. Soc. Rev.*, 2011, **40**, 5122; K. Kohler, S. S. Prockl and W. Kleist, *Curr. Org. Chem.*, 2006, **10**, 1585; P. J. Guiry and D. Kiely, *Curr. Org. Chem.*, 2004, **8**, 781; G. T. Crisp, *Chem. Soc. Rev.*, 1998, **27**, 427; W. Cabri and I. Candiani, *Acc. Chem. Res.*, 1995, **28**, 2; J. W. Ruan and J. L. Xiao, *Acc. Chem. Res.*, 2011, **44**, 614; R. F. Heck, *Acc. Chem. Res.*, 1979, **12**, 146.
  - 2 J. Le Bras and J. Muzart, *Chem. Rev.*, 2011, **111**, 1170.
  - 3 C. G. Jia, T. Kitamura and Y. Fujiwara, *Acc. Chem. Res.*, 2001, **34**, 844; J. L. Wu, X. L. Cui, L. M. Chen, G. J. Jiang and Y. J. Wu, *J. Am. Chem. Soc.*, 2009, **131**, 13888; T. Yokota, M. Tani, S. Sakaguchi and Y. Ishii, *J. Am. Chem. Soc.*, 2003, **125**, 1476; S. H. Cho, S. J. Hwang and S. Chang, *J. Am. Chem. Soc.*, 2008, **130**, 9254; M. Yu, Y. J. Xie, C. S. Xie and Y. H. Zhang, *Org. Lett.*, 2012, **14**, 2164; Q. Zhang, H. Z. Yu, Y. T. Li, L. Liu, Y. Huang and Y. Fu, *Dalton T.*, 2013, **42**, 4175.
  - 4 T. Nishikata, A. R. Abela and B. H. Lipshutz, *Angew. Chem., Int. Ed.*, 2010, **49**, 781; T. Nishikata and B. H. Lipshutz, *J. Am. Chem. Soc.*, 2009, **131**, 12103; S. Narayan, J. Muldoon, M. G. Finn, V. V. Fokin, H. C. Kolb and K. B. Sharpless, *Angew. Chem., Int. Ed.*, 2005, **44**, 3275; V. G. Zaitsev and O. Daugulis, *J. Am. Chem. Soc.*, 2005, **127**, 4156.
  - 5 E. M. Ferreira, H. M. Zhang and B. M. Stoltz, *Tetrahedron*, 2008, **64**, 5987; M. Ludwig, S. Stromberg, M. Svensson and B. Akerman, *Organometallics*, 1999, **18**, 970; J. Koubachi, S. Berteina-Raboin, A. Mouaddib and G. Guillaumet, *Synthesis-Stuttgart*, 2009, 271.
  - 6 J. L. Zhao, L. H. Huang, K. Cheng and Y. H. Zhang, *Tetrahedron Lett.*, 2009, **50**, 2758; P. Li, J. W. Gu, Y. Ying, Y. M. He, H. F. Zhang, G. Zhao and S. Z. Zhu, *Tetrahedron*, 2010, **66**, 8387; M. R.

- Luzung, C. A. Lewis and P. S. Baran, *Angew. Chem., Int. Ed.*, 2009, **48**, 7025.
- 7 J. Tsuji, H. Nagashima, *Tetrahedron*, 1984, **40**, 2699; M. D. K. Boele, G. P. F. van Strijdonck, A. H. M. de Vries, P. C. J. Kamer, J. G. de Vries and P. W. N. M. van Leeuwen, *J. Am. Chem. Soc.*, 2002, **124**, 1586; Y. Yokoyama, K. Tsuruta and Y. Murakami, *Heterocycles*, 2002, **56**, 525.
- 8 D. H. Wang, K. M. Engle, B. F. Shi and J. Q. Yu, *Science*, 2010, **327**, 315; B. F. Shi, Y. H. Zhang, J. K. Lam, D. H. Wang and J. Q. Yu, *J. Am. Chem. Soc.*, 2010, **132**, 460.
- 10 K. M. Engle, D. H. Wang and J. Q. Yu, *Angew. Chem., Int. Ed.*, 2010, **49**, 6169.
- 10 P. A. Enquist, P. Nilsson, P. Sjöberg, M. Larhed, *J. Org. Chem.*, 2006, **71**, 8779; Q. Zhang, H.-Z. Yu, Y.-T. Li, L. Liu, Y. Huang and Y. Fu., *Dalton Trans.*, 2013, **42**, 4175; Z. Li, Y. Fu, S.-L. Zhang, Q.-X. Guo and L. Liu, *Chem-Asian J.*, 2010, **5**, 1475.
- 15 11 X. Chen, K. M. Engle, D. H. Wang and J. Q. Yu, *Angew. Chem., Int. Ed.*, 2009, **48**, 5094.
- 12 H. Zhou, Y. H. Xu, W. J. Chung and T. P. Loh, *Angew. Chem., Int. Ed.*, 2009, **48**, 5355; W. Rauf, A. L. Thompson and J. M. Brown, *Chem. Commun.*, 2009, 3874; H. Zhou, W. J. Chung, Y. H. Xu and T. P. Loh, *Chem. Commun.*, 2009, 3472; D. H. Wang, T. S. Mei and J. Q. Yu, *J. Am. Chem. Soc.*, 2008, **130**, 17676; e) C. Y. Wang, I. Piel and F. Glorius, *J. Am. Chem. Soc.*, 2009, **131**, 4194; A. Bartoszewicz and B. Martin-Matute, *Org. Lett.*, 2009, **11**, 1749.
- 25 13 X. Chen, C. E. Goodhue and J. Q. Yu, *J. Am. Chem. Soc.*, 2006, **128**, 12634; K. L. Hull and M. S. Sanford, *J. Am. Chem. Soc.*, 2007, **129**, 11904; B. F. Shi, N. Mangel, Y. H. Zhang and J. Q. Yu, *Angew. Chem., Int. Ed.*, 2008, **47**, 4882; K. Parthasarathy and C. H. Cheng, *J. Org. Chem.*, 2009, **74**, 9359; W. W. Jin, Z. K. Yu, W. He, W. Ye and W. J. Xiao, *Org. Lett.*, 2009, **11**, 1317; S. G. Lim, J. A. Ahn and C. H. Jun, *Org. Lett.*, 2004, **6**, 4687; g) A. Garca-Rubia, R. Gomez Arrayas and J. C. Carretero, *Angew. Chem., Int. Ed.*, 2009, **48**, 6511; P. Melnyk, B. Legrand, J. Gasche, P. Ducrot and C. Thal, *Tetrahedron*, 1995, **51**, 1941.
- 30 14 A. Vigalok, O. Uzan, L. J. W. Shimon, Y. Ben-David, J. M. L. Martin and D. Milstein, *J. Am. Chem. Soc.*, 1998, **120**, 12539; M. Montag, L. Schwartsburd, R. Cohen, G. Leitus, Y. Ben-David, J. M. L. Martin and D. Milstein, *Angew. Chem., Int. Ed.*, 2007, **46**, 1901; M. Blug, H. Heuclin, T. Cantat, X. F. Le Goff, N. Mezaillies and P. Le Floch, *Organometallics*, 2009, **28**, 1969; R. Samanta and A. P. Antonchick, *Angew. Chem., Int. Ed.*, 2011, **50**, 5217; D. Shabashov and O. Daugulis, *J. Am. Chem. Soc.*, 2010, **132**, 3965.
- 35 15 E. W. Werner and M. S. Sigman, *J. Am. Chem. Soc.*, 2010, **132**, 13981; M. M. S. Andappan, P. Nilsson, H. von Schenck and M. Larhed, *J. Org. Chem.*, 2004, **69**, 5212; Z. H. He, S. Kirchberg, R. Fröhlich and A. Studer, *Angew. Chem., Int. Ed.*, 2012, **51**, 3699; J. W. Ruan, X. M. Li, O. Saidi and J. L. Xiao, *J. Am. Chem. Soc.*, 2008, **130**, 2424; A. S. Tsai, M. Brasse, R. G. Bergman and J. A. Ellman, *Org. Lett.*, 2011, **13**, 540.
- 40 16 C. G. Jia, W. J. Lu, T. Kitamura and Y. Fujiwara, *Org. Lett.*, 1999, **1**, 2097; M. Tani, S. Sakaguchi and Y. Ishii, *J. Org. Chem.*, 2004, **69**, 1221; N. P. Grimster, C. Gauntlett, C. R. A. Godfrey and M. J. Gaunt, *Angew. Chem., Int. Ed.*, 2005, **44**, 3125; A. Maehara, T. Satoh and M. Miura, *Tetrahedron*, 2008, **64**, 5982; Y. Z. Yang, K. Cheng and Y. H. Zhang, *Org. Lett.*, 2009, **11**, 5606.
- 45 17 M. L. Steigerwald and W. A. Goddard III, *J. Am. Chem. Soc.*, 1984, **106**, 308; A. K. Rappé *Organometallics*, 1990, **9**, 466.
- 18 L. Zhang and D. C. Fang, *J. Org. Chem.*, 2013, **78**, 2405.
- 50 19 M. Boudart in *Kinetics of Chemical Processes*, Prentice-Hall Englewood Cliffs, New Jersey, 1968, pp. 63; R. Weston Jr and H. A. Schwarz in *Chemical Kinetics*, Prentice-Hall Englewood Cliffs, New Jersey, 1972, pp. 17–20.
- 55 20 G. Cai, Y. Fu, Y. Li, X. Wan and Z. Shi, *J. Am. Chem. Soc.*, 2007, **129**, 7666.
- 60 21 J.-J. Li, T.-S. Mei and J.-Q. Yu, *Angew. Chem., Int. Ed.*, 2008, **47**, 6452.
- 22 F. A. Carey, R. J. Sundberg in *Advanced Organic Chemistry*, Vol. B, Springer-Verlag, New York, 2007, pp. 389–459.
- 70 23 M. D. K. Boele, G. P. F. van Strijdonck, A. H. M. de Vries, P. C. J. Kamer, J. G. de Vries and P. W. N. M. van Leeuwen, *J. Am. Chem. Soc.*, 2002, **124**, 1586; J. R. Wang, C. T. Yang, L. Liu and Q.-X. Guo, *Tetrahedron Lett.*, 2007, **48**, 5449; C. E. Houlden, C. D. Bailey, J. G. Ford, M. R. Gagne, G. C. Lloyd-Jones and K. I. Booker-Milburn, *J. Am. Chem. Soc.*, 2008, **130**, 10066.
- 75 24 M. J. Frisch, G. W. Trucks, H. B. Schlegel, G. E. Scuseria, M. A. Robb, J. R. Cheeseman, G. Scalmani, V. Barone, B. Mennucci, G. A. Petersson, H. Nakatsuji, M. Caricato, X. Li, H. P. Hratchian, A. F. Izmaylov, J. Bloino, G. Zheng, J. L. Sonnenberg, M. Hada, M. Ehara, K. Toyota, R. Fukuda, J. Hasegawa, M. Ishida, T. Nakajima, Y. Honda, O. Kitao, H. Nakai, T. Vreven, J. A. Montgomery, Jr., J. E. Peralta, F. Ogliaro, M. Bearpark, J. J. Heyd, E. Brothers, K. N. Kudin, V. N. Staroverov, R. Kobayashi, J. Normand, K. Raghavachari, A. Rendell, J. C. Burant, S. S. Iyengar, J. Tomasi, M. Cossi, N. Rega, J. M. Millam, M. Klene, J. E. Knox, J. B. Cross, V. Bakken, C. Adamo, J. Jaramillo, R. Gomperts, R. E. Stratmann, O. Yazyev, A. J. Austin, R. Cammi, C. Pomelli, J. W. Ochterski, R. L. Martin, K. Morokuma, V. G. Zakrzewski, G. A. Voth, P. Salvador, J. J. Dannenberg, S. Dapprich, A. D. Daniels, O. Farkas, J. B. Foresman, J. V. Ortiz, J. Cioslowski and D. J. Fox, *Gaussian 09, Revision A.02*, Gaussian, Inc., Wallingford CT, 2009.
- 80 25 N. Godbout, D. R. Salahub, J. Andzelm and E. Wimmer, *Can. J. Chem.*, 1992, **70**, 560; C. Sosa and C. Lee, *J. Phys. Chem.*, 1992, **96**, 6630.
- 85 26 G. Scalmani, M. J. Frisch and J. Chem. Phys. 2010, **132**, 114110.
- 90 27 G. Y. Tao, W. H. Mu, G. A. Chass, T. H. Tang and D. C. Fang, *Int. J. Quantum Chem.*, 2013, **113**, 975; D. C. Fang, *SCRF-RADII program*, Beijing Normal University, Beijing, China, free of charge for academic users.
- 95 28 K. Fukui, *Acc. Chem. Res.*, 1981, **14**, 363; H. P. Hratchian and H. B. Schlegel, *J. Chem. Phys.*, 2004, **120**, 9918; H. P. Hratchian and H. B. Schlegel, *J. Chem. Theor. Comput.*, 2005, **1**, 61.
- 100 29 D. C. Fang, *THERMO program*, Beijing Normal University, Beijing, China, free of charge for academic users.
- 105 30 Y. Zhao, D. G. Truhlar, *Theor. Chem. Acc.*, 2008, **120**, 215; Y. Zhao, D. G. Truhlar, *J. Phys. Chem.*, 2006, **110**, 5121; R. Peverati, D. G. Truhlar, *J. Phys. Chem. Lett.*, 2011, **2**, 2810.
- 110 31 R. F. W. Bader in *Atoms in Molecules: A Quantum Theory*, Oxford University Press, Oxford, UK, 1990.
- 115 32 D.-C. Fang and T.-H. Tang, *AIM98PC*, Beijing Normal University, Beijing, China, 1998.
- 120 33 *AIMPAC*, available from Professor Bader's Laboratory, McMaster University, Hamilton, Ontario, Canada.

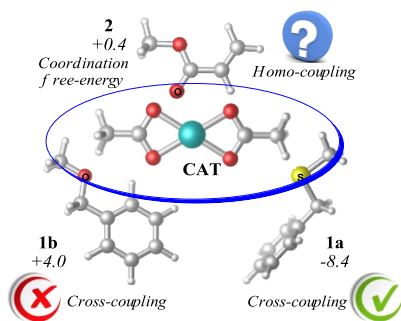
Cite this: DOI: 10.1039/c0xx00000x

www.rsc.org/xxxxxx

ARTICLE TYPE

## Entry for the Table of Contents

Two competing reaction pathways for the dehydrogenative Heck couplings have been found. The property of the directing groups on reactants will determine the dominance of these two pathways.



10